Published May 11, 2017

Original Research

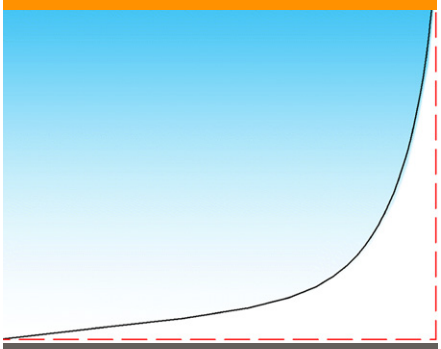

Derivation and Validation of a New Soil Pore-Structure-Dependent Flux–Saturation Relationship

DongHao Ma, JiaBao Zhang,* and YunXuan Lu

Recently, a method based on the soil water flux (F)–saturation (Θ) relationship, $F(\Theta)$, assumed to be independent of time and soil properties, has become an important technique to simplify solving Richards' equation so as to develop a simple, rapid, and low-cost approach to estimate soil hydraulic properties. However, the actual $F(\Theta)$ is soil pore-structure dependent. So far, there exists no theory that can provide a specific functional form of soil pore-structure-dependent $F(\Theta)$. In this research, we derived a general soil moisture profile function and then a general expression of $F(\Theta)$: $F = \Theta[1 + a_2(1 - \Theta^{1/a_2})]$. The only parameter in $F(\Theta)$, a_2, is a function of the initial soil water saturation and the soil pore structure index that reflects the shape of the soil water retention curve. Infiltration experiments with three test soils and four actual soils were conducted to test the proposed relationships. The results verified the independence of $F(\Theta)$ on time at small time scales. The results also indicated that the derived formula predicted $F(\Theta)$ in good agreement with what was measured for all test soils under different initial soil moisture conditions. In addition, the upper and lower limit curves of $F(\Theta)$ calculated by the proposed formula were consistent with the theoretical curves. Compared with other empirical relationships, the new formula was the best for describing the theoretical upper limit curve of $F(\Theta)$. Furthermore, the new theoretical relationship was also found to be appropriate for horizontal absorption. Generally, the developed relationship is more accurate and helpful to solve Richards' equation.

Core Ideas

- A soil pore-structure-dependent soil water flux–saturation relationship $F(\Theta)$ was derived.
- This $F(\Theta)$ depends on the shape coefficient of soil water retention curve and initial saturation.
- This $F(\Theta)$ is simple and accurate for constant-saturation infiltration and absorption.

D.H. Ma, J.B. Zhang, and Y.X. Lu, State Experimental Station of Agro-Ecosystem in Fengqiu, State Key Lab. of Soil and Sustainable Agriculture, Institute of Soil Science, Chinese Academy of Sciences, Nanjing 210008, People's Republic of China; Y.X. Lu, College of Resource and Environmental Sciences, Nanjing Agriculture Univ., Nanjing 210095, People's Republic of China. *Corresponding author (jbzhang@issas.ac.cn).

Received 25 Nov. 2016.
Accepted 7 Mar. 2017.

Citation: Ma, D.H., J.B. Zhang, and Y.X. Lu. 2017. Derivation and validation of a new soil pore-structure-dependent flux–saturation relationship. Vadose Zone J. 16(5). doi:10.2136/vzj2016.11.0117

Vol. 16, Iss. 5, 2017

Complete soil hydraulic properties are important basic conditions for modeling soil hydrological processes with the Richards equation. Thanks to sizable progress in computational techniques, currently it is not difficult to numerically solve a complex hydrological model. However, quick, accurate, and low-cost determination of the required soil hydraulic properties is still a problem. Indirect methods based on monitoring the soil hydraulic process and inverse modeling are some of the most promising approaches satisfying such requirements. Normally, the inversion refers to numerical inversions. However, for the interactive non-convergence and non-uniqueness of numerical inversions, the inversions based on approximate solutions have been key research topics during the past several decades. To achieve a good inversion approach, one needs to derive a simple and accurate approximation of an analytical solution to the Richards equation under a specific condition. Nevertheless, solving Richards' equation analytically is not easy without appropriate assumptions. This is one of the reasons why it remains one of the most interesting topics for soil physical researchers (Assouline, 2013; Basha, 2011; Caputo and Stepanyants, 2008; Hogarth et al., 2013; Triadis and Broadbridge, 2010, 2012). A recent example included a novel analytical solution to the Richards equation, developed for estimating the soil moisture profile to the meter depth from P-band radar remote sensing measurements (Sadeghi et al., 2017).

In the past several decades, various infiltration models have been derived from the Richards equation (Assouline, 2013). However, they have failed to accurately estimate even the most commonly used soil hydraulic properties such as saturated hydraulic conductivity and sorptivity (Valiantzas, 2010). The recently proposed solutions (Basha, 2011; Caputo and Stepanyants, 2008; Hogarth et al., 2013; Triadis and Broadbridge, 2010) may be

accurate for simulating infiltration but too complex to be used for estimating soil hydraulic properties. Therefore, simpler solutions are required for determining soil hydraulic properties.

Important progress resulted from finding that the soil water flux–saturation relation was almost independent of time at small time (White, 1979; White et al., 1979) and dependent on relative soil water saturation with simple functions (Evangelides et al., 2005; Philip, 1973; Vauclin and Haverkamp, 1985). Philip (1973) found that the assumption concerning the soil water flux–saturation relation can be used to greatly simplify solving Richards' equation (Philip, 1973). Following this finding, many interactive or approximate analytical solutions (Barry et al., 1995; Boulier et al., 1984; Haverkamp et al., 1990; Hogarth et al., 2013; Knight and Philip, 1973; Parlange et al., 1997; Philip and Knight, 1974) have been proposed with similar assumptions. Recently, two new approximate solutions (Ma et al., 2009, 2015) were derived for horizontal and vertical infiltration into soils. They are simple and accurate enough that they can be used for determining soil hydraulic properties through inversions. The important progress in Ma et al. (2009, 2015) is that a simple function independent of soil texture or a soil pore structure index was used to describe the flux–saturation relationship. Unfortunately, we still do not have a full understanding of the characteristics of the flux–saturation relationship, especially its general mathematical expression. Further insights into the flux–saturation relationship may help to further improve the analytical solutions and thus the estimation accuracy of soil hydraulic properties from simple infiltration experiments with the inversion methods based on them as in Ma et al. (2009, 2016).

The conception of the flux–saturation relationship was first proposed by McWhorter (1971) and defined as the relation between the relative soil water flux F and the relative soil water saturation Θ. According to the definitions of Philip (1973), for vertical infiltration

$$F=\frac{J_w-K_i}{J_{w0}-K_i} \quad [1]$$

$$\Theta=\frac{\theta-\theta_i}{\theta_0-\theta_i} \quad [2]$$

where J_{w0} and J_w are the soil water flux at the surface and at any depth (cm min^{-1}), respectively, K_i is the soil hydraulic conductivity corresponding to the initial soil water content (cm min^{-1}), θ_i is the initial soil water content (cm^3 cm^{-3}), θ_0 is the soil water content at the surface (cm^3 cm^{-3}), and θ is the soil water content at depth z (cm^3 cm^{-3}).

Since the flux–saturation method was first used by Philip (1973) to solve the Richards equation, many functions have been explicitly adopted to describe the soil water flux–saturation relationship $F(\Theta)$. There are also some functions concerning $F(\Theta)$ that have been implicitly used in solving infiltration problems (Vauclin and Haverkamp, 1985). Generally, these functions of $F(\Theta)$ can be used for both vertical and horizontal infiltration and can be classified into three types (Table 1). Type I is the constant type (Parlange, 1971; Philip, 1955), representing a uniform flux distribution independent of Θ. Normally, this type approximately holds only when the soil moisture profile is close to saturation. Type II is the saturation-dependent type where F is a function of Θ without any parameters (Boulier et al., 1984; Brutsaert, 1976; Dirksen, 1975; Parlange, 1975; Philip, 1973; Smiles et al., 1982; White et al., 1979). This type of $F(\Theta)$represents curves only for specific soils, such as linear soils or "delta-function" soils (Philip, 1973) and has been adopted mostly as a common relationship to simplify the processes of solving Richards' equations. Type III is the saturation and soil pore-structure-dependent type where F is a function of Θ with a parameter for soil properties (Evangelides et al., 2005; Kutílek, 1980). This type of $F(\Theta)$ is more flexible and can simulate soil water flux–saturation relationships with higher accuracy for soils with a broad texture range or soil structure state (Evangelides et al., 2005). Review of the various types of $F(\Theta)$ and comparisons between them have been presented by Evangelides et al. (2005) and Vauclin and Haverkamp (1985). The

Table 1. Three types (I, constant; II, saturation-dependent function; and III, saturation and soil pore structure dependent function) of the flux–saturation relationship function $F(\Theta)$ proposed in the literature (mainly recompiled from Evangelides et al. [2005] and Vauclin and Haverkamp [1985]).

Type	$F(\Theta)$	Notes†	References
I	$\pi/4$		Philip (1955)
	1		Parlange (1971)
II	$\exp[-\text{inverfc}(\Theta)^2]$	theoretical upper limit	Philip (1973)
	$\sin[(\pi/2)\Theta^{\pi/4}]$	a good approximation to $\exp[-\text{inverfc}(\Theta)^2]$	White et al. (1979)
	Θ	theoretical lower limit	Philip (1973)
	$\Theta^{1/2}$		Brutsaert (1976)
	$\Theta^{2-4/\pi}$		White et al. (1979)
	$\Theta^{2-\pi/2}$		Dirksen (1975)
	$[\pi/(2+2\gamma)]\Theta^{1-\gamma}$	$\gamma = 0.67$	Dirksen (1975)
	$2\Theta/(\Theta+1)$		Parlange (1975)
	$1-(1-\Theta)^{1.19}$		Smiles et al. (1982)
	$1-(1-\Theta)^{1.06}$		Boulier et al. (1984)
III	Θ^{β}	upper limit with $\beta = 0.46$ lower limit with $\beta = 1$	Kutílek (1980) $\beta = 0.8$
	$1-(1-\Theta)^{n}$	upper limit with $n = 2.36$ lower limit with $n = 1$	Evangelides et al. (2005) $n = 1.149$–1.389
	$2\Theta-[1-(1-\Theta)^{m}]$	upper limit with $m = 0.5$ lower limit with $m = 1$	Evangelides et al. (2005) $m = 0.718$–0.867

† Upper limit and lower limit refer to the limits of the possible curves of $F(\Theta)$; β, m, and n are soil pore-structure-dependent factors but constants for a specific soil at short time scales. The optimum values of the parameters for upper and lower limit curves were obtained by comparing with the theoretical limit curves.

higher accuracy of the approximate solutions to infiltration problems improved by $F(\Theta) = \Theta$ (Type II) relative to $F(\Theta) = 1$ (Type I), as well as the superiority of $F(\Theta) = \Theta^{\beta}$ (Type III) over $F(\Theta) = \Theta$ (Type II) have been verified by Kutílek (1980). There is no doubt that the use of the appropriate Type III $F(\Theta)$ can help to obtain better approximate solutions for the determination of soil hydraulic properties.

Although the Type III $F(\Theta)$ maybe more accurate and flexible in its ability to describe soil pore-structure dependency or texture dependency, no researchers have used them to solve infiltration problems. One of the important reasons is that there is an additional parameter in the Type III $F(\Theta)$ compared with Type I and Type II. Apart from the theoretical upper and lower limits of the possible actual curves of $F(\Theta)$ (Philip, 1973), so far there is still no theory that can explain the soil pore-structure-dependent behavior of $F(\Theta)$ for general soils. All three of the Type III $F(\Theta)$ listed in Table 1 are empirical formulas. We do not know exactly what the relationships of their parameters to soil hydraulic properties are or how to determine them. Thus, the objective of this study was to theoretically derive a new Type III soil water flux–saturation $F(\Theta)$ and to find out the significant physical meaning of the parameter so as to ease its determination.

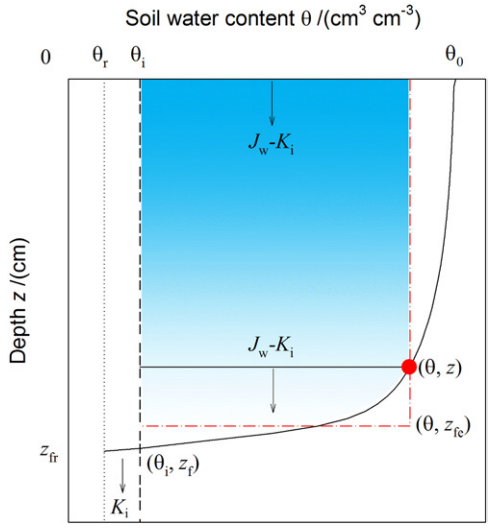

Fig. 1. Schematic diagram of a soil moisture profile and the extended Green–Ampt assumption, where J_w is the soil water flux and K_i is the soil hydraulic conductivity corresponding to the initial soil water content, which transforms to the traditional Green–Ampt assumption if the red point is fixed at $(\theta_0, 0)$. The variables θ_r and θ_i are residual and initial soil water content, respectively; θ_0 is soil water content at the water inlet; and z_f, z_{fe}, and z_{fr} are actual, effective, and virtual wetting front depths, respectively, among which z_{fe} is the function of specific soil water content.

Theory

Method I

Green and Ampt (1911) proposed a piston-type water content profile with a well-defined wetting front for water infiltration into a homogeneous soil with uniform antecedent water content under a constant ponding depth. According to this assumption, soils are saturated down to the wetting front, where the water content drops abruptly to the initial water content. Because the actual soil moisture profile (solid line in Fig. 1) is not a piston type, the equivalent wetting front depth (z_{fe}) for the Green–Ampt model is always less than the actual wetting front depth (z_f). The traditional Green–Ampt assumption can be exhibited as a special case of the dash-dotted lines in Fig. 1, that is, the red point is moved to the soil surface along the wetting front and fixed at $(\theta_0, 0)$. Thus, the traditional Green–Ampt assumption is usually used for the whole soil moisture profile. Here, we extend the assumption to part of the water content profile ranging from the initial soil water content θ_i to any soil water content θ (dash-dotted lines in Fig. 1). According to capillary theory, the total water fluxes in the capillary tubes saturated at soil water content θ are the same from the soil surface to depth z. In addition, we make another assumption that the soil moisture profile can be described by a simple function. For the following derivation, we also define a variable for the virtual wetting front depth z_{fr} that refers to the depth at which the extended curve of the soil moisture profile function intersects the residual water content (cm^3 cm^{-3}), θ_r.

According to the mean-value theorem for integrals, the actual water stored between z and z_{fr} can be expressed as

$$\int_{z(\theta)}^{z_{fr}} (\theta - \theta_r)\,dz = \xi(\theta - \theta_r)(z_{fr} - z) \quad [3]$$

where z is the vertical distance from the soil surface (cm), and ξ is a variable between 0.5 and 1 representing the proportion of the shaded zone in the rectangle enclosed by the long dashed lines in Fig. 2a. If we assume that ξ is a constant independent of z, the two sides of Eq. [3] can be differentiated with respect to z. After rearrangement,

$$\frac{d\theta}{\theta - \theta_r} = -\frac{(1/\xi - 1)\,dz}{z_{fr} - z} \quad [4]$$

Integrating the left side of Eq. [4] from the surface water content θ_0 (cm^3 cm^{-3}) to the water content θ (cm^3 cm^{-3}) at depth z and the right side of Eq. [4] from 0 to z, the non-piston-type soil water content distribution can be obtained after rearrangement:

$$S = \frac{\theta - \theta_r}{\theta_0 - \theta_r} = \left(1 - \frac{z}{z_{fr}}\right)^a = \left(1 - b\frac{z}{z_f}\right)^a \quad [5]$$

where S is the soil water saturation, θ_0 is the soil water content at the water inlet (cm^3 cm^{-3}), $b = z_f/z_{fr}$, and $a = 1/\xi - 1$. Because S is equal to the initial soil water saturation, S_i at the wetting front z_f, $b = 1 - S_i^{1/a}$ can be derived as another form of b. If ξ is independent of z, a will also be independent of z.

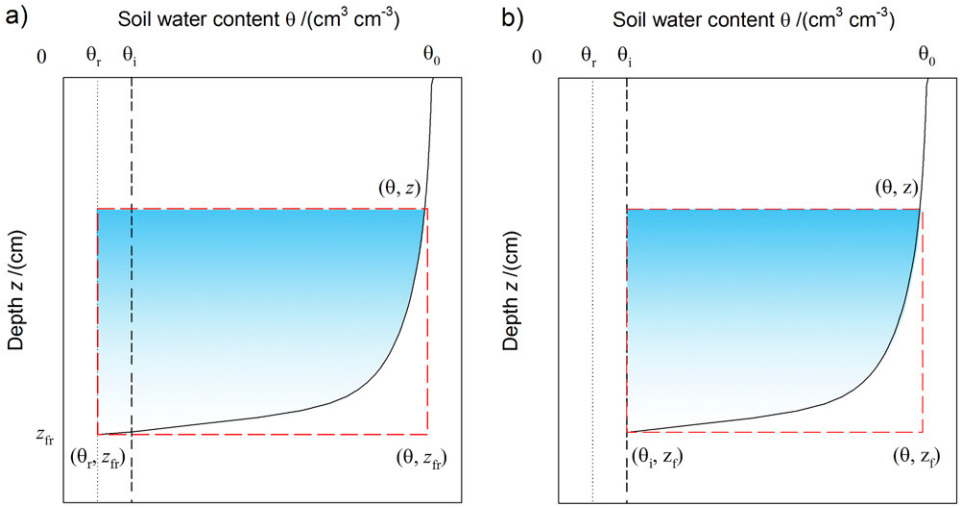

Fig. 2. Schematic diagrams of the two assumptions made in (a) Eq. [3] and (b) Eq. [19]. The proportion of the shaded zone in the rectangle enclosed by the long dashed lines was assumed to be a constant, which should be between 0.5 and 1. The variables θ, θ_r, and θ_i are the specific, residual, and initial soil water contents, respectively; θ_0 is soil water content at the water inlet; and z_f and and z_{fr} are actual and virtual wetting front depths, respectively.

According to Philip (1957a), the shape of the soil moisture profile is developed very early and changes very slightly after infiltration starts. Thus, a time-independent a is also expected. Combining knowledge of the soil moisture profile shape, the range of the values of a should be (0, 1). The lower limit represents "delta-function" soils (i.e., $a = 0$) and the upper limit represents linear soils (i.e., $a = 1$). Equation [5] was also found by Ma et al. (2015) and Wang et al. (2002), with Richards' equation and the Brooks–Corey hydraulic model (Brooks and Corey, 1964), and gave consistent simulations with the measured horizontal and vertical soil moisture profiles. However, here, no specific hydraulic property model is used, which means that the results in this research need not be limited by the function type of the soil hydraulic property models.

The cumulative water flux I_w (cm) through the section with water content θ is

$$I_w = \int_{\theta_i}^{\theta} z\,\mathrm{d}\theta + K_i t = (\theta - \theta_i) z_{fe} + K_i t \qquad [6]$$

where θ_i is the initial water content (cm^3 cm^{-3}), K_i is the soil hydraulic conductivity corresponding to the initial water content (cm min^{-1}), t is the infiltration time (min), and z_{fe} is the effective wetting front depth when a saturated wet zone is assumed.

The depth of the ponded water on the soil surface is usually far less than the average matric pressure head, and it is not difficult to add it into the equation. Thus, it is ignored here for convenience. With the assumption of a piston-type profile for the partial wetting front (Fig. 1), according to Darcy's law, the soil water flux at one depth can be expressed as (Green and Ampt, 1911)

$$J_w = \frac{\mathrm{d}I_w}{\mathrm{d}t} = K_e\left(1 + \frac{s_f}{z_{fe}}\right) \qquad [7]$$

where K_e is the effective hydraulic conductivity of the partial moisture profile (cm min^{-1}) and s_f is the average matric pressure head at the partial wetting front (cm) representing the range from θ_i to θ. Both K_e and s_f should be functions of θ.

For the non-piston-type soil moisture profile, the cumulative water flux at one depth can also be obtained by substituting Eq. [5] into [6]:

$$I_w = \int_{\theta_i}^{\theta} z\,\mathrm{d}\theta + K_i t = U z_f + K_i t \qquad [8]$$

where

$$U = \frac{\theta_0 - \theta_r}{(a+1)b}\left[\left(a + 1 - aS^{1/a}\right)S - (1+ab)S_i\right] \qquad [9]$$

Comparing Eq. [6] and [8], we can obtain the relationship between effective and actual wetting front positions:

$$z_{fe} = \frac{U}{\theta - \theta_i} z_f \qquad [10]$$

Defining z_{fe0} as the effective wetting front depth when the red point in Fig. 1 is fixed at (θ_0, 0), the ratio of z_{fe} for the range (θ_i, θ) to z_{fe0} for (θ_i, θ_0) is deduced as an expression independent of time:

$$\frac{z_{fe}}{z_{fe0}} = \frac{\theta_0 - \theta_i}{\theta - \theta_i}\frac{U}{U_0} \qquad [11]$$

where U_0 is U when S is equal to 1, that is

$$U_0 = \frac{\theta_0 - \theta_r}{(a+1)b}\left[1 - (1+ab)S_i\right] \qquad [12]$$

With a method similar to that of Prevedello et al. (2009), we obtain the two relationships (Appendix A):

$$K_e = \frac{U}{U_0}(K_{e0} - K_i) + K_i \qquad [13]$$

$$s_f = \frac{K_{e0}}{K_e}\frac{\theta_0-\theta_i}{\theta-\theta_i}\left(\frac{U}{U_0}\right)^2 s_{fe0} \quad [14]$$

where K_{e0} and s_{fe0} are the effective hydraulic conductivity of the whole soil moisture profile (cm min^{-1}) and the average matric pressure head at the whole wetting front (cm), respectively.

With Eq. [7], [11], [13], and [14], the flux–saturation relation F can be obtained as a function of water saturation S:

$$\begin{aligned} F(S) &= \frac{J_w - K_i}{J_{w0} - K_i} \\ &= \frac{K_e - K_i}{K_{e0} - K_i} \\ &= \frac{\left(a+1-aS^{1/a}\right)S-(1+ab)S_i}{1-(1+ab)S_i} \end{aligned} \quad [15]$$

or a function of relative saturation Θ

$$\begin{aligned} F(\Theta) = &\frac{1}{1-(1+ab)S_i} \\ &\times\left\{(a+1)(1-S_i)\Theta - a\left[(1-S_i)\Theta+S_i\right]^{1/a+1}\right. \\ &\left.+a(1-b)S_i\right\} \end{aligned} \quad [16]$$

where J_{w0} is the soil water flux at the surface (cm min^{-1}).

When $a \to 0$ and $b \to 1$, Eq. [16] gives the lower limit of the flux–saturation relationship curves:

$$F(\Theta) = \Theta \quad [17]$$

When $a = 1$ and $b = 1 - S_i$, the upper limit of the curves can be obtained from Eq. [16]:

$$F(\Theta) = \Theta(2-\Theta) \quad [18]$$

Method II

Applying the mean-value theorem for integrals to the increased water storage between z and the actual wetting front z_f, we get

$$\int_{z(\theta)}^{z_f}(\theta-\theta_i)\,dz = \eta(\theta-\theta_i)(z_f - z) \quad [19]$$

where η is a variable between 0.5 and 1, representing the proportion of the shaded zone in the rectangle enclosed by the long dashed lines in Fig. 2b. Similarly, we assume that η is a depth- and time-independent constant according to Philip (1957a). Following the same steps as in Method I, we can derive another equation describing the soil moisture profile

$$\Theta = \frac{\theta-\theta_i}{\theta_0-\theta_i} = \left(1-\frac{z}{z_f}\right)^{a_2} \quad [20]$$

where $a_2 = 1/\eta - 1$, and then

$$U_0 = \frac{\int_{\theta_i}^{\theta} z\,d\theta}{z_f} = \frac{\theta_0-\theta_i}{a_2+1} \quad [21]$$

Equation [20] was derived by Wang et al. (2003) by solving Richards' equation (Richards, 1931) with the Brooks–Corey hydraulic model (Brooks and Corey, 1964). With the same steps for deducing Eq. [15], the new expression for describing the flux–saturation relationship $F(\Theta)$ is obtained:

$$F(\Theta) = \Theta\left[1+a_2\left(1-\Theta^{1/a_2}\right)\right] \quad [22]$$

Equation [22] is simpler than Eq. [16] in form but has another parameter different from a. The only parameter, a_2, may depend on the initial soil water saturation. Combining Eq. [12] and [21], it is not difficult to derive the parameter a_2 as a function of a and the initial soil water saturation:

$$a_2 = \frac{ab-(1-b)(1-S_i)}{1-(ab+1)S_i} \quad [23]$$

where $b = 1 - S_i^{1/a}$ from Eq. [5] because $S = S_i$ when $z = z_f$. Similar to a, the range of the values of a_2 is (0, 1).

Similarly, Eq. [22] also defines the upper and lower limits of the flux–saturation relation curves. The upper limit curve is exactly the same as Eq. [18], and the lower limit curve is the same as Eq. [17] derived from Eq. [16].

Using the method proposed above, the theoretical flux–saturation relationship during horizontal absorption into general soils can also be deduced with simpler processes than that above (see Appendix B). The relationship $F(\Theta)$ and its upper and lower limits for horizontal absorption show the same functional form as for vertical infiltration as well as the soil moisture profile.

Materials and Methods

Experimental Procedures

Infiltration experiments with seven soils (three test soils and four actual soils) were conducted to test the relationships proposed above. The three test soils (a sandy soil, a loamy soil, and a clay soil) were taken from the typical soils (Carsel and Parrish, 1988) in the HYDRUS-1D software, with the hydraulic parameters of the Brooks–Corey model (Brooks and Corey, 1964) listed in Table 2. The infiltration data were generated numerically by

Table 2. Typical soil hydraulic properties, including the residual and saturated soil water content (θ_r and θ_s, respectively), empirical parameters in the Brooks–Corey model (α and n_{BC}, Brooks and Corey, 1964), the saturated hydraulic conductivity (K_s), and a parameter reflecting soil pore tortuosity (l) of the three test soils used in simulated vertical infiltration experiments (data from Carsel and Parrish, 1988).

Soil	θ_r	θ_s	α	n_{BC}	K_s	l
	——$cm^3\ cm^{-3}$——		cm^{-1}		$cm\ min^{-1}$	
Sand	0.020	0.417	0.1380	0.592	0.350	2
Loam	0.027	0.434	0.0897	0.220	0.022	2
Clay	0.090	0.385	0.0254	0.137	0.001	2

the HYDRUS-1D software package, Version 3.0 (Šimůnek et al., 2005). The soil columns were 60 cm long. A constant water content (saturated) was used for the upper boundary condition and free drainage for the lower boundary condition in simulations. For each soil, four simulations were performed corresponding to four different initial soil water contents (0.03, 0.15, 0.25, and 0.35 $cm^3\ cm^{-3}$ for the sandy soil; 0.04, 0.12, 0.25, and 0.35 $cm^3\ cm^{-3}$ for the loamy soil; and 0.12, 0.25, 0.33, and 0.36 $cm^3\ cm^{-3}$ for the clay soil) to test the dependency of a and a_2 on the initial soil water saturation. The cumulative fluxes at the soil surface and soil moisture profiles vs. time were used as data for the tests below. The wetting front advance was obtained from the simulated time-lapse soil moisture profiles.

The other four soils were Chengang loam (10.6% clay, 45.5% silt, and 43.9% sand), Lizhuang loam (17.6% clay, 39.1% silt, and 43.3% sand), Pandian sandy loam (18.3% clay, 16.2% silt, and 55.5% sand) and Daheigang sand (6.3% clay, 4.5% silt, and 89.2% sand) sampled from the 0- 20-cm depth in Fenqiu County in North China. The field bulk densities were 1.35 g cm^{-3} for Chengang loam, 1.51 g cm^{-3} for Daheigang sand, and 1.4 g cm^{-3} for Lizhuang loam and Pandian sandy loam. The sampled soils were air dried and sieved to determine the soil particle distribution according to the US soil texture classification (sand 50–2000 μm, silt 2–50 μm, and clay 0–2 μm). Soil particles below 2 mm in diameter were used for the infiltration experiments. Air-dry soils were weighed and uniformly packed into a plastic column that was 50 cm long and composed of 10 small rings with a height of 5 cm and an inner diameter of 3 cm. The soil packing was made in 5-cm height increments to ensure the homogeneity of the soil in the columns. Vertical infiltration and horizontal absorption experiments were conducted for each soil. The ponded infiltration and absorption experiments were performed, separately, with a 1.2-cm surface water head and 1-cm water head at the water inlet supplied by mariotte tubes. During the experiments, the cumulative infiltration or absorption and the visually observed wetting front advance with time were recorded. Just after the end of infiltration or absorption, the soil column was separated into 10 sections. The soil moisture content of the upper and lower parts of each section were sampled and measured using the gravimetric method. Because we used a destructive sampling method, experiments with three durations were conducted to obtain soil moisture distributions at three different times. Each treatment was replicated three times. The soil water contents of the first layer saturated by water and the last layer not yet wetted were taken as θ_0 and θ_i, respectively. The residual water content, θ_r, was estimated as the soil water content at −1.5 MPa.

Calculation of the Flux–Saturation Relationship

From the Measured Soil Moisture Profile

According to the definition of F by Philip (1973), the flux–saturation relationship F for one-dimensional vertical infiltration can be derived in another form (Knight and Philip, 1973). Similar to the approach used by White (1979) for absorption, the time-average F can be calculated from two observed soil moisture profiles:

$$F=\frac{\int_{\theta_i}^{\theta}\left(\partial z/\partial t\right)_\theta \mathrm{d}\theta}{\int_{\theta_i}^{\theta_0}\left(\partial z/\partial t\right)_\theta \mathrm{d}\theta}\approx\frac{\sum_{\theta_i}^{\theta}\left[z_{t_2}\left(\theta_k\right)-z_{t_1}\left(\theta_k\right)\right]}{\sum_{\theta_i}^{\theta_0}\left[z_{t_2}\left(\theta_k\right)-z_{t_1}\left(\theta_k\right)\right]} \quad [24]$$

where z_{t1} and z_{t2} are the soil moisture profiles at times t_1 and t_2, respectively, and θ_k is the integral variable of soil water content.

Normally, the measured soil moisture profiles are obtained by measurements at some fixed depths and are not smooth because of errors in sampling and measurement. To calculate F, the observed soil moisture profiles need to be smoothed using some manual, numerical, or analytical method, e.g., the empirical equation proposed by Evangelides et al. (2005). In this study, we used Eq. [5] to smooth the moisture profiles. For the smoothed profile, it is convenient to use the inverse function of Eq. [5] to calculate the depths corresponding to the soil water contents θ_k with a fixed step on profiles.

From the Observed Infiltration Process

Using the methods developed above, the time-average soil water flux–saturation relation curves were also calculated by Eq. [16] or [22] with initial soil saturation and the shape coefficient of the soil moisture profile a or a_2. Least square optimization was used to estimate the needed parameters a and a_2. Normally, K_i is negligible for low initial soil moisture, and then the cumulative surface water flux (i.e., cumulative infiltration) can be expressed as a linear function of the wetting front advance according to Eq. [8]:

$$I_{w0}=U_0 z_f \quad [25]$$

Given I_{w0} and z_f vs. time, θ_r, θ_i, and θ_0, U_0 can be obtained by the least-square linear regression of Eq. [25] of the data of I_{w0} vs. z_f. The parameter a can be obtained by numerically solving Eq. [12], which is an implicit function of a. Because the values of b ($b = 1 - S_i^{1/a}$) are very close to 1 when $S_i \to 0$, we can assume $b = 1$ in our infiltration experiments for simplicity. Then, we can obtain a and a_2 by solving Eq. [12] and [21], that is

$$a \approx \frac{\theta_0 - \theta_i - U_0}{U_0 + \theta_i - \theta_r} \quad [26]$$

$$a_2 = \frac{\theta_0 - \theta_i - U_0}{U_0} \quad [27]$$

Results and Discussion

As an example, Chengang loam was chosen to show how to calculate $F(\Theta)$ from the measured soil moisture profile, which is the same for vertical infiltration and horizontal absorption. The first step is to use Eq. [5] to fit or smooth the measured soil moisture profiles at three times (Fig. 3) to acquire the corresponding coefficients. The low root mean square errors (RMSE) between fitted and measured data in Fig. 3 indicate that Eq. [5] is good at smoothing the observed soil moisture profiles. The depths corresponding to the soil water contents θ_k with a fixed step on profiles [e.g., $(\theta_0 - \theta_i)/30$] were calculated by inverting Eq. [25] with the coefficients obtained above. Then, it is convenient to calculate the average $F(\Theta)$ between any two times using Eq. [24] with the smoothed soil moisture profiles at the two times.

Time-lapsed I_{w0} vs. z_f were observed during infiltration. The value $U_0 = 0.386$ was obtained as the slope of the linear regression of Eq. [25] to the data of I_{w0} vs. z_f, which fit well, as indicated by the high coefficient of determination r^2 (Fig. 4). Because $\theta_r = 0$, $\theta_i = 0.018$ cm^3 cm^{-3}, and $\theta_0 = 0.45$ cm^3 cm^{-3}, it can be calculated that $a = 0.113$ and $a_2 = 0.118$ from Eq. [26] and [27], respectively.

Soil Moisture Profile

An assumption was made in Eq. [3] that the coefficient ξ is a constant for a specific soil. If this assumption is true, the shape coefficient a (i.e., $1/\xi - 1$) should not depend on the initial soil water content. The same is the case for the shape coefficient a_2 (i.e., $1/\eta - 1$), which should depend on a but may also depend on the initial soil water saturation for the integral range of Eq. [19] that varies with θ_i. The results shown in Fig. 5 justify these assumptions. No significant tendency can be found for the values of a with increased initial soil water contents for any of the three test soils. However, the values of a_2 show a great dependency on a and the initial saturation S_i. The value of a_2 drops to a as S_i decreases to zero. The increase in a_2 with a and initial saturation S_i can be well estimated by Eq. [23]. It is reasonable to conclude that a may depend only on the basic properties of a soil, such as soil texture and structure, and thus can be taken as one of the comprehensive indicators reflecting soil properties.

Shown in Fig. 6 and 7 are the soil moisture profiles during vertical infiltration and horizontal absorption into four actual soils, measured and calculated using Eq. [5] and [20]. The results show a good agreement between the calculated soil moisture profiles from Eq. [5] and [20] and the measured profiles for both infiltration and absorption processes. In fact, Eq. [5] and [20] have also been derived by other researchers (Ma et al., 2009, 2015; Wang et al., 2003) and tested using numerical experiments. Wang et al. (2003) deduced the same equation as Eq. [20] with an approximate analytical approach and found it suitable to describe the soil moisture profile during constant-head infiltration. Ma et al. (2009, 2015) derived Eq. [5], as well as a simple function linking a to the shape coefficient of the soil water retention curve described by the Brooks–Corey model (Brooks and Corey, 1964). In their research, the ability of Eq. [5] was confirmed to accurately describe soil moisture profiles of the three test soils in Table 2 during infiltration and absorption under different initial moisture contents (e.g., Fig. 4–6 in Ma et al. [2009] and Fig. 2 in Ma et al. [2015]).

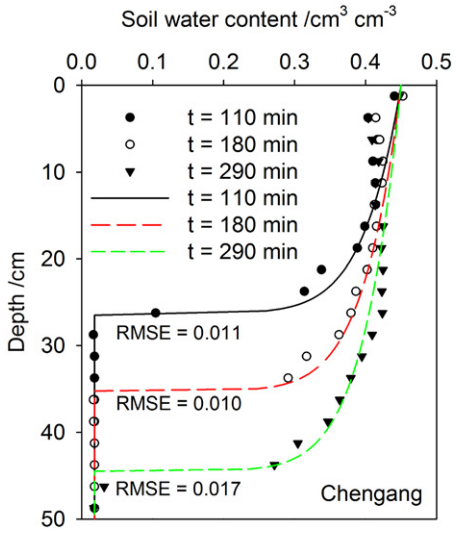

Fig. 3. Measured points and lines fitted by Eq. [5] for soil moisture profiles of Chengang loam at three times during vertical infiltration; RMSE is the root mean square error between measured and fitted soil moisture contents of the soil profile.

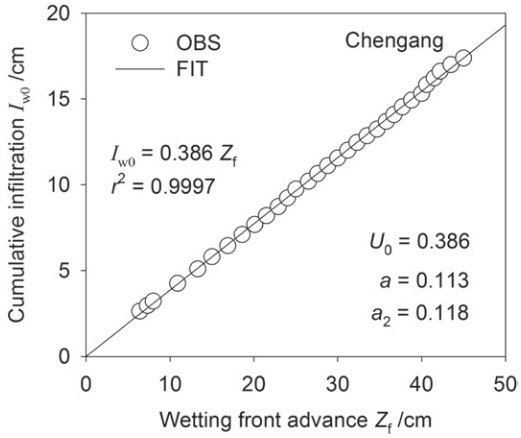

Fig. 4. Observed (OBS) and fitted by Eq. [25] (FIT) cumulative infiltration vs. wetting front advance of Chengang loam; r^2 is the coefficient of determination of the linear regression, U_0 is the average soil moisture increase, and a and a_2 are shape coefficients.

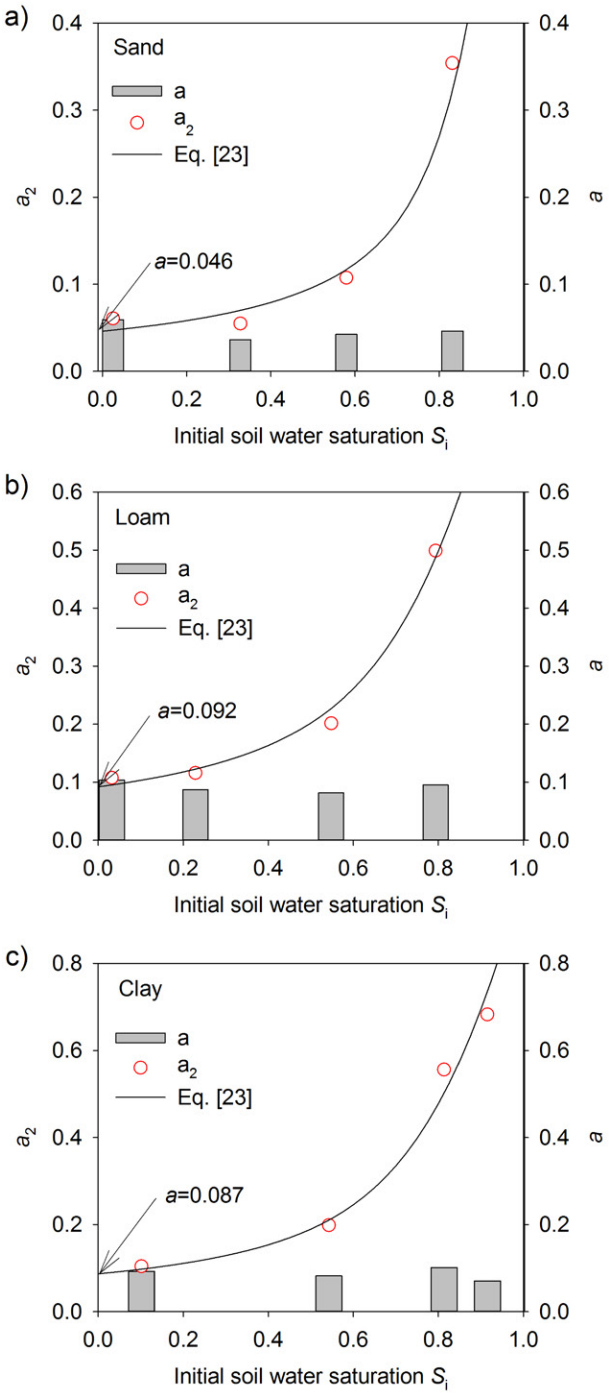

Fig. 5. The actual (symbols) and predicted (by Eq. [23], line) relations between the shape coefficients (a and a_2) of the soil moisture profile and initial water saturation for three test soils: (a) sand, (b) loam, and (c) clay. The actual values of a and a_2 were calculated using Eq. [26] and [27], respectively, and from the average soil moisture increase, U_0, which was obtained by fitting Eq. [25] to cumulative infiltration vs. wetting front advance.

Flux–Saturation Relationship

Shown in Fig. 8 are the $F(\Theta)$ curves for three soil types (sand, loam, and clay) with different initial soil water contents as simulated by Eq. [16] compared with the simulations by HYDRUS-1D. For a better differentiation between the $F(\Theta)$ curves of the different treatments, soil water saturation S rather than Θ was chosen as the horizontal coordinate. The results indicate that the $F(\Theta)$ curves calculated by Eq. [16] are coincident with those by Eq. [22] for all three test soils with different initial soil water contents. Both Eq. [16] and [22] predicted $F(\Theta)$ curves generally in agreement with those simulated by HYDRUS-1D. The possible reason is that the wetting front behavior is more complex for a heavy soil, which deviates further from the piston-type assumption of the Green–Ampt model.

For the four actual soils, the results in Fig. 9 and 10 also confirmed the suitability of the above assumptions and the effectiveness of the derived flux–saturation relationships. As shown in Fig. 9, the calculated $F(\Theta)$ curves from the measured infiltration processes exhibit few changes with infiltration time but depend on soil type. All the curves are between the theoretical upper and lower limits calculated by Eq. [17] and [18]. The curve is closer to the upper limit for a coarse soil (e.g., Daheigang) but to the lower limit for a fine soil (e.g., Chengang). Additionally, no obvious difference can be found between the curves calculated by Eq. [16] and [22]. Both of them produced $F(\Theta)$ curves in agreement with the results calculated from the measured soil moisture profiles. Because Eq. [22] is simpler than Eq. [16] in form and the parameter of the former has a clear relationship (Eq. [23]) with that of the latter and the initial soil moisture state, it is possible to replace Eq. [16] with Eq. [22] for modeling $F(\Theta)$. In addition, the values of a and a_2 tend to increase when the soil texture gets coarser (Table 3). These results are consistent with the theoretical analysis by Ma et al. (2015). The case is the same for horizontal absorption shown in Fig. 10 and Table 3.

According to the theoretical analysis by Philip (1973), the relationship $F(\Theta)$ during infiltration may vary with time and boundary conditions, and all the curves will converge to the lower limit $F = \Theta$ for long time periods. However, $F(\Theta)$ depended little on time in our experiments, as well as in the observed results during constant-flux infiltration by White (1979). Thus, at least for short time periods, $F(\Theta)$ can be considered independent of time. The theoretical lower limit of $F(\Theta)$ deduced here is the same as that proposed by Philip (1973). Because of the simplicity of the relation $F = \Theta$ and no other appropriate expressions, $F = \Theta$ is most commonly used in solving infiltration problems under different boundary conditions. The theoretical upper limit of $F(\Theta)$ for constant-saturation absorption was proposed by Philip (1973), and the simple approximation $F = \sin[(\pi/2)\Theta^{\pi/4}]$ was given by White et al. (1979). Because matric potential overcomes gravitational potential on water movement during short time periods, infiltration is close to absorption. The approximation $F = \sin[(\pi/2)\Theta^{\pi/4}]$ may also be an upper limit of $F(\Theta)$ for constant-saturation infiltration. As shown in Fig. 9 and 10, the upper limit curve described by Eq. [18] is below $F = \sin[(\pi/2)\Theta^{\pi/4}]$. At least in our experiments, no measured curve was found

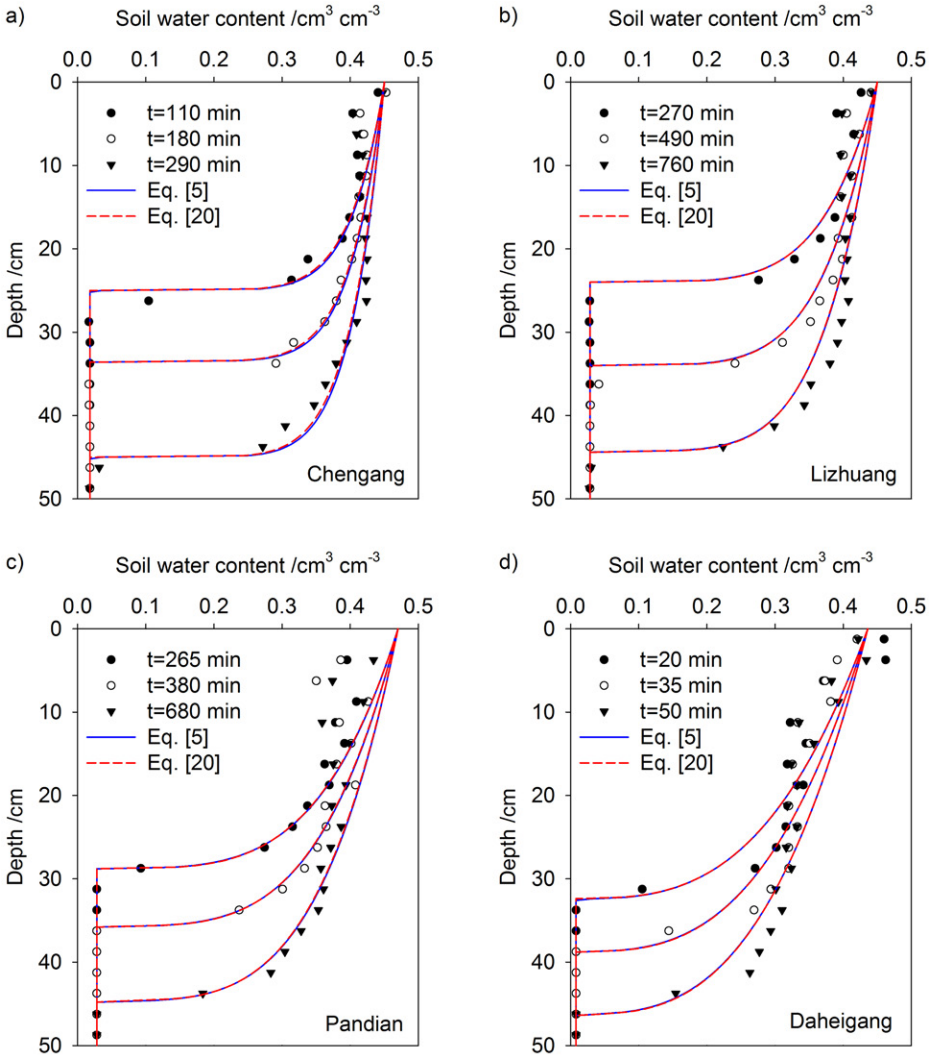

Fig. 6. Measured (points) and calculated (lines) soil moisture profiles by Eq. [5] and [20] using measured wetting front depth and shape coefficient a obtained from the observed infiltration process during vertical infiltration into four actual soils: (a) Chengang, (b) Lizhuang, (c) Pandian, and (d) Daheigang.

outside the range between the curves described by Eq. [17] and [18]. It is possible that the actual flux–saturation relation curves have a narrower range than that proposed by Philip (1973).

It is interesting to discuss and compare the ability of the Type III functions to describe the upper and lower limit curves of $F(\Theta)$. When the values of the parameters β, n, and m are equal to 1, all three of the Type III empirical functions converge to the theoretical lower limit curve $F = \Theta$. However, the upper limit curves differ much from the theoretical upper limit curve $F = \sin[(\pi/2)\Theta^{\pi/4}]$. When optimization techniques were used to obtain the parameter values of the empirical functions by fitting the curve $F = \sin[(\pi/2)\Theta^{\pi/4}]$, the upper limit curves were found as $F = \Theta^{0.46}$ for $F = \Theta^{\beta}$, $F = 1 - (1 - \Theta)^{2.36}$ for $F = 1 - (1 - \Theta)^{n}$, and $F = 2\Theta - [1 - (1 - \Theta)^{0.5}]$ for $F = 2\Theta - [1 - (1 - \Theta)^{m}]$. As shown in Fig. 11, $F = \Theta^{0.46}$ overestimated F in the range of low saturation but underestimated F in the range of high saturation. Conversely, $F = 2\Theta - [1 - (1 - \Theta)^{0.5}]$ underestimated F in the range of low saturation but greatly overestimated F in the range close to saturation; $F = 1 - (1 - \Theta)^{2.36}$ gave a very good estimation of F across the whole range. The best estimation came from $F = \Theta[1 + 2(1 - \Theta^{1/2})]$, that is, Eq. [22] with $a_2 = 2$. It can be concluded that $F = \Theta^{\beta}$ and $F = 2\Theta - [1 - (1 - \Theta)^{m}]$ are not good functions of $F(\Theta)$ for the soils with water diffusivity far from the "delta-function" type. Equation [22] and $F = 1 - (1 - \Theta)^{n}$ seem to be more appropriate functional forms for describing actual flux–saturation curves of general soils. However, superior to the empirical function $F = 1 - (1 - \Theta)^{n}$, Eq. [22] was derived theoretically and its parameter a_2 has a physical meaning, i.e., it represents the shape coefficient of the soil moisture profile.

In our theoretical results, the relationship $F(\Theta)$ for horizontal absorption shows the same functional form as vertical infiltration, as well as the soil moisture profile. However, this result does not imply that horizontal absorption and vertical infiltration have the same $F(\Theta)$ for a given soil because the parameter a in Eq. [16] has different relationships to the shape coefficient of soil water retention curve for horizontal absorption and vertical infiltration, that is

$$a = \frac{n_{BC}}{2n_{BC} + 2} \qquad [28]$$

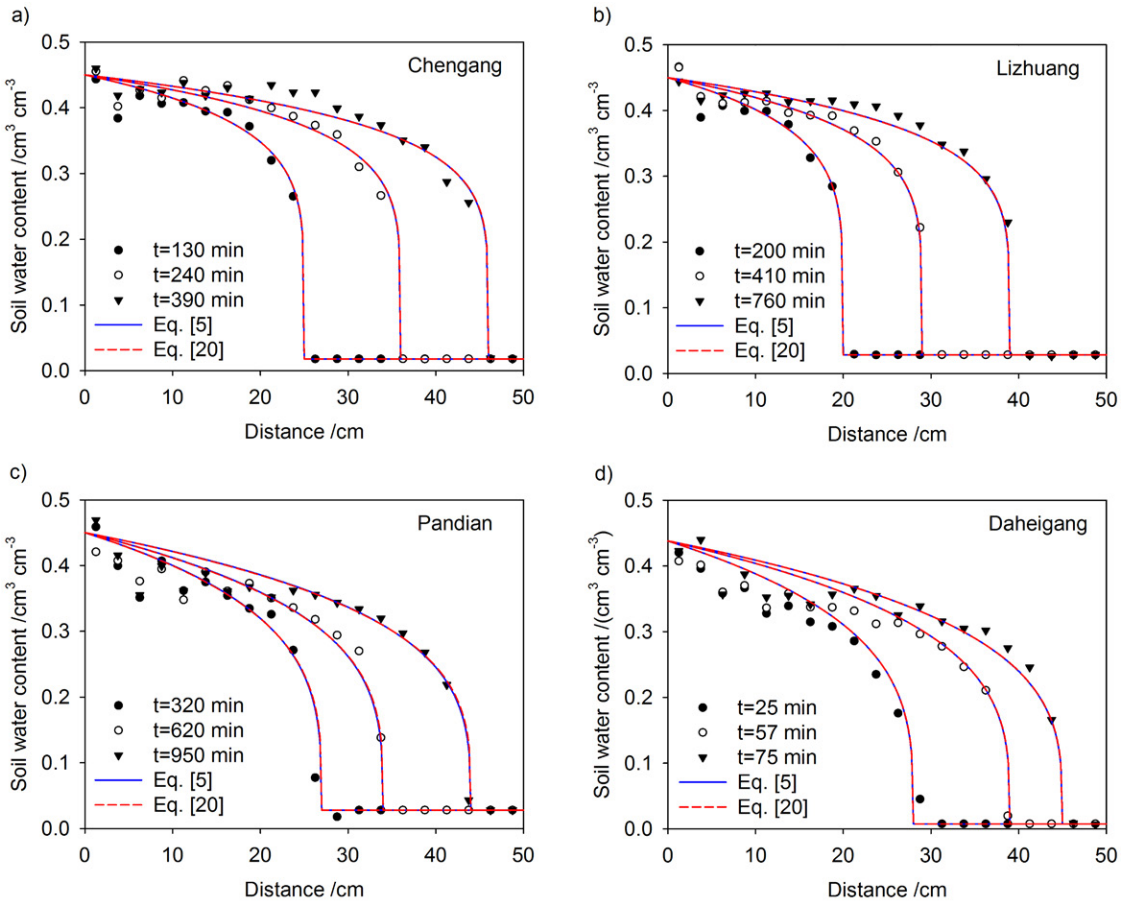

Fig. 7. Measured (points) and calculated (lines) soil moisture profiles by Eq. [5] and [20] using measured wetting front depth and shape coefficient a obtained from the observed infiltration process during horizontal absorption into four actual soils: (a) Chengang, (b) Lizhuang, (c) Pandian, and (d) Daheigang.

derived by Ma et al. (2015) for vertical infiltration and

$$a = \frac{n_{BC}}{2n_{BC}+1} \quad [29]$$

derived by Ma et al. (2009) for horizontal absorption, where n_{BC} is a soil pore structure index controlling the shape of the soil water retention curve in the Brooks–Corey model (Brooks and Corey, 1964). Shown in Fig. 12 are the comparisons of a vs. n_{BC} obtained from measured or simulated data (23 soils for vertical infiltration and 28 soils for horizontal absorption) by Ma et al. (2009, 2015, 2016) and predicted by Eq. [28] and [29] from n_{BC}. Equations [28] and [29] show an increase of a with n_{BC} for both infiltration and absorption. As depicted in Fig. 12, the curve predicted by Eq. [29] is in good agreement with the measured data for horizontal absorption. The measured data of a vs. n_{BC} for vertical infiltration show a large deviation from the curve predicted by Eq. [28]. The uncertainty in determining wetting front locations, especially during vertical infiltration, should be responsible for this deviation. For example, heterogeneous flows even in the disturbed soils can result in a deeper wetting front depth during infiltration. The setup of a spatial discretization step and the threshold of soil moisture content tend to produce a shallower wetting front depth from numerically simulated data. They can partially explain why the actual four soils have obviously greater a values (Table 3) than the three test soils (Fig. 5). The other possible reasons include that the derived functions, Eq. [5] and [20], are too simple to accurately describe the part of the actual soil moisture profile at the wetting front. Finally, the Brooks–Corey model used in the numerical simulations is more appropriate for coarser soils and does not describe soil water retention curves very well close to saturation (van Genuchten, 1980). Even so, there is no doubt that Eq. [28] generally predicted the main variation tendency of a with n_{BC} (Fig. 12), especially for horizontal absorption. Equations [16], [28], and [29] indicate that $F(\Theta)$ is a function that depends only on the soil pore-structure index and initial soil water saturation for both infiltration and absorption under constant-saturation boundary conditions.

Summary and Conclusions

The soil water flux–saturation relationship $F(\Theta)$ can be used as an effective technique to greatly simplify the solution of Richards' equation, which has recently found great use in estimating soil hydraulic properties. However, theoretical formulas are scarce for

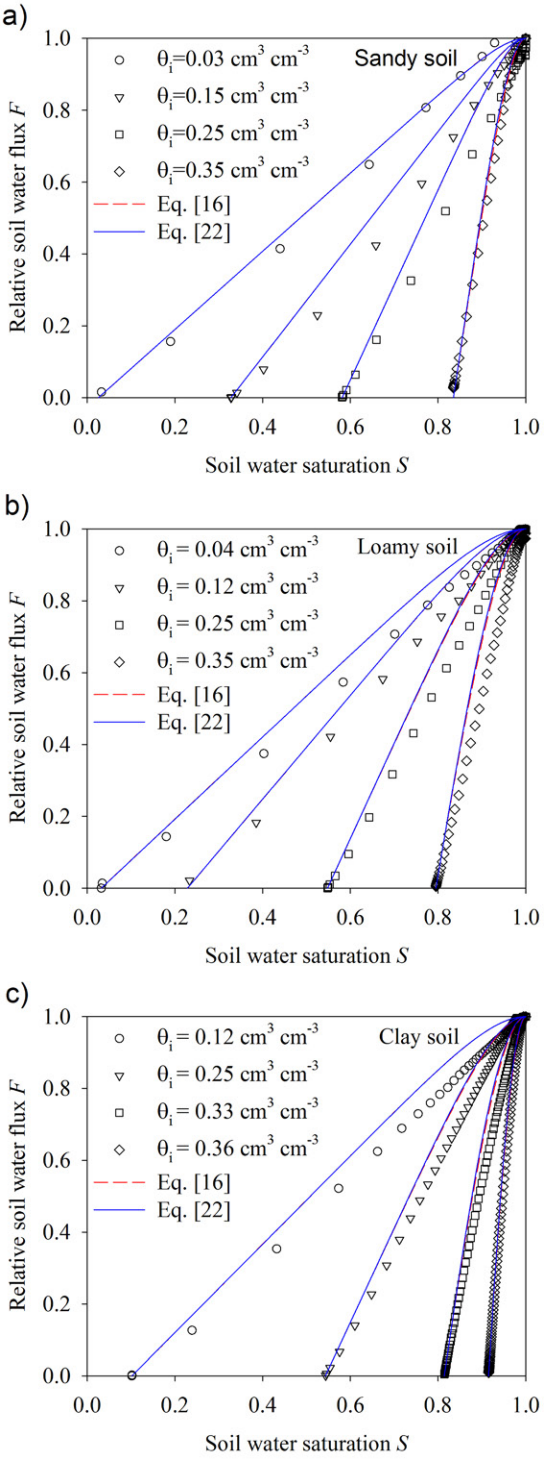

Fig. 8. Comparisons between the soil water flux–saturation relationships calculated by Eq. [16] and [22] using the shape coefficient *a* obtained from the observed infiltration process (lines) and simulated by HYDRUS-1D (symbols) for infiltration into three test soils with different initial soil water contents θ_i: (a) sand, (b) loam, (c) clay.

describing soil properties dependent on $F(\Theta)$. In this research, we theoretically derived a formula for $F(\Theta)$, which shows that $F(\Theta)$ depends only on soil pore structure and initial soil water saturation for both constant-saturation infiltration and absorption. The proposed relationships were proved effective by numerical and experimental data describing the dependence of $F(\Theta)$ on soil properties. These relationships are superior to other empirical equations reviewed by Evangelides et al. (2005), which use parameters with no significant physical meaning, and thus nowadays no methods are available to determine them independently. Based on these new relationships, it is possible in the future to obtain better approximate solutions of infiltration processes under constant-saturation boundary conditions for improving the estimation of soil hydraulic properties by indirect methods.

Appendix A

Similar to the process of deriving the traditional Green–Ampt model (Green and Ampt, 1911), the implicit relationship between the effective wetting front depth and time can be obtained from Eq. [6] and [7]:

$$(K_e - K_i)t = (\theta - \theta_i)z_{fe} - (\theta - \theta_i)R_f \ln\left(1 + \frac{z_{fe}}{R_f}\right) \quad [A1]$$

where

$$R_f = \frac{K_e s_f}{K_e - K_i} \quad [A2]$$

When $z = 0$, Eq. [A1] transforms to the traditional Green–Ampt model:

$$(K_{e0} - K_i)t = (\theta_0 - \theta_i)z_{fe0} - (\theta_0 - \theta_i)R_{f0} \ln\left(1 + \frac{z_{fe0}}{R_{f0}}\right) \quad [A3]$$

where

$$R_{f0} = \frac{K_{e0} s_{f0}}{K_{e0} - K_i} \quad [A4]$$

Express t in Eq. [A1] in terms of a polynomial of z_{fe} and subsequently invert that polynomial to z as a power series of $t^{j/2}$ ($j = 1, 2, 3, \ldots$) (Prevedello et al., 2009) to compare with the series solution proposed by Philip (1957b). Then Eq. [A1] can be rewritten as an explicit function of time:

$$\begin{aligned} z_{fe} = {} & \left(2\frac{K_e - K_i}{\theta - \theta_i}R_f\right)^{1/2} t^{1/2} + \frac{1}{3}\left(2\frac{K_e - K_i}{\theta - \theta_i}\right)t \\ & + \frac{1}{18}\left[2\left(\frac{K_e - K_i}{\theta - \theta_i}\right)^3 \frac{1}{R_f}\right]^{1/2} t^{3/2} \\ & + \frac{1}{135}\left[2\left(\frac{K_e - K_i}{\theta - \theta_i}\right)^2 \frac{1}{R_f}\right] t^2 \\ & + \frac{1}{1080}\left[2\left(\frac{K_e - K_i}{\theta - \theta_i}\right)^5 \frac{1}{{R_f}^3}\right]^{1/2} t^{5/2} + \ldots \end{aligned} \quad [A5]$$

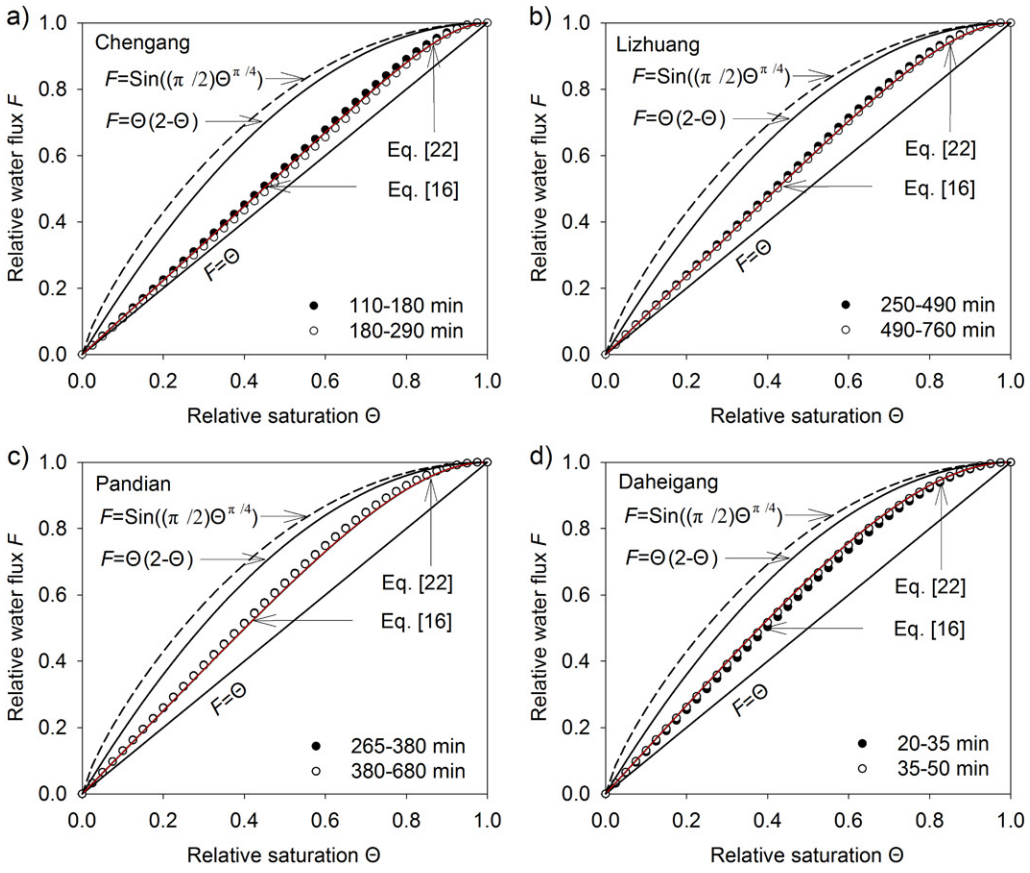

Fig. 9. Comparisons between the soil water flux–saturation relationships calculated by Eq. [24] from measured soil moisture profiles (symbols) and by Eq. [16] and [22] using the shape coefficient *a* obtained from the observed infiltration process (lines) during vertical infiltration into four actual soils: (a) Chengang, (b) Lizhuang, (c) Pandian, and (d) Daheigang.

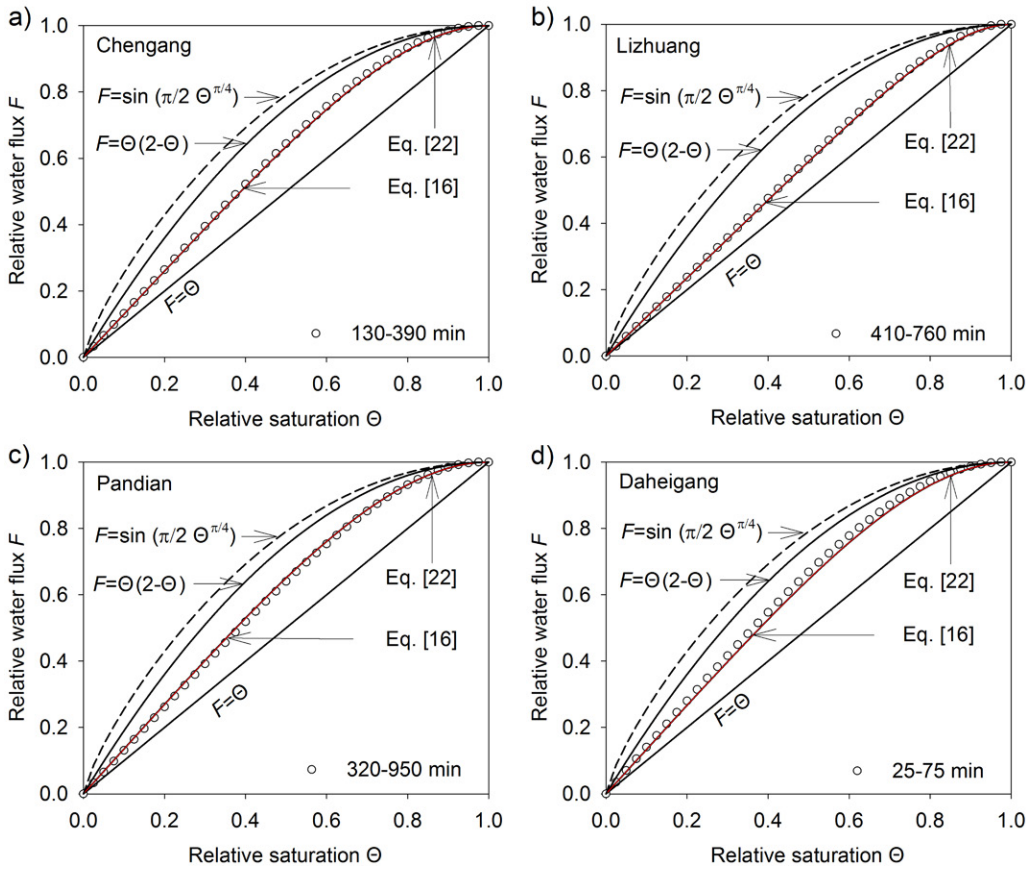

Fig. 10. Comparisons between the soil water flux–saturation relationships calculated by Eq. [24] from measured soil moisture profiles (symbols) and by Eq. [16] and [22] using the shape coefficient *a* obtained from the observed infiltration process (lines) during horizontal absorption into four actual soils: (a) Chengang, (b) Lizhuang, (c) Pandian, and (d) Daheigang.

Table 3. Physical properties of four actual soils and the corresponding values of shape coefficients of the soil moisture profile, a and a_2, for Methods I and II determined by Eq. [26] and [27], respectively, from the infiltration process for vertical infiltration or horizontal absorption and coefficients of determination for the linear regression of Eq. [25] to the observed data of cumulative infiltration or absorption vs. wetting front advance (r_1^2 and r_2^2).

		Vertical infiltration			Horizontal absorption		
Site	Texture	r_1^2	a	a_2	r_2^2	a	a_2
Chengang	loam	1.000	0.113	0.118	0.999	0.160	0.168
Lizhuang	loam	0.999	0.171	0.185	0.999	0.165	0.178
Pandian	sandy loam	0.999	0.234	0.253	0.999	0.253	0.275
Daheigang	sand	0.999	0.329	0.326	0.996	0.274	0.281

Similarly, Eq. [A3] can be rewritten as

$$z_{fe0}=\left(2\frac{K_{e0}-K_i}{\theta_0-\theta_i}R_{f0}\right)^{1/2}t^{1/2}+\frac{1}{3}\left(2\frac{K_{e0}-K_i}{\theta_0-\theta_i}\right)t+\frac{1}{18}\left[2\left(\frac{K_{e0}-K_i}{\theta_0-\theta_i}\right)^3\frac{1}{R_{f0}}\right]^{1/2}t^{3/2}+\frac{1}{135}\left[2\left(\frac{K_{e0}-K_i}{\theta_0-\theta_i}\right)^2\frac{1}{R_{f0}}\right]t^2+\frac{1}{1080}\left[2\left(\frac{K_{e0}-K_i}{\theta_0-\theta_i}\right)^5\frac{1}{R_{f0}^3}\right]^{1/2}t^{5/2}+\ldots \quad [A6]$$

The ratio of any two terms in Eq. [A5] and [A6] with the same order should then be equal to the right side of Eq. [11]. Here, we take only the first two terms of Eq. [A5] and [A6] as approximations to Eq. [A1] and [A3], respectively. Letting the ratio of the second terms of Eq. [A5] and [A6] be equal to the right side of Eq. [11], we then have

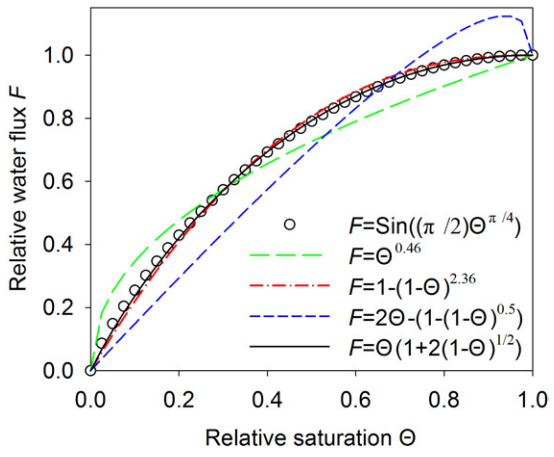

Fig. 11. Comparisons of the upper limit curves of several flux–saturation functions (lines) with the theoretical upper limit curve (circle). Except the last one, the parameter values of the Type III empirical functions were obtained by fitting them to the theoretical upper limit curve $F=\sin[(\pi/2)\Theta^{\pi/4}]$.

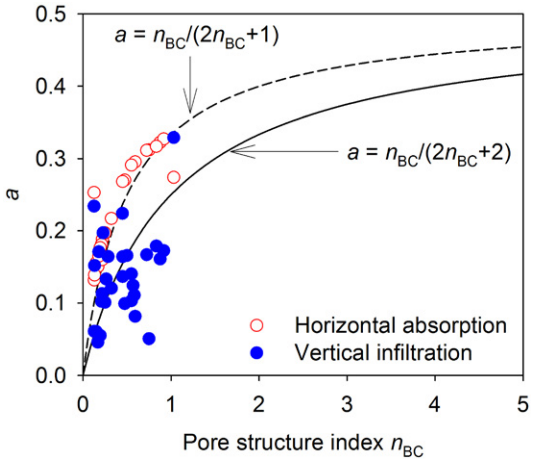

Fig. 12. Comparisons of shape coefficient a vs. the Brooks–Corey soil pore structure index n_{BC} obtained from cumulative infiltration or absorption vs. wetting front advance (points) and those predicted by Eq. [28] and [29] from n_{BC} (lines). The data for horizontal absorption for 28 soils are from Ma et al. (2009, 2016). The data for vertical infiltration are from Ma et al. (2015) and numerical simulations by HYDRUS-1D used the same 19 soils as Ma et al. (2009, Table 1).

$$K_e=\frac{U}{U_0}(K_{e0}-K_i)+K_i \quad [A7]$$

Combining with Eq. [A7] and letting the ratio of the first terms of Eq. [A5] and [A6] be equal to the right side of Eq. [11] gives

$$s_f=\frac{K_{e0}}{K_e}\frac{\theta_0-\theta_i}{\theta-\theta_i}\left(\frac{U}{U_0}\right)^2 s_{f0} \quad [A8]$$

Appendix B

Derivation of the Flux–Saturation Relationship for Horizontal Absorption

Method I

With similar assumptions and derivations as made for Method I for infiltration, it is not difficult to obtain Eq. [B1] for describing the soil moisture profile during horizontal absorption:

$$S=\left[1-\left(1-S_i^{1/a}\right)\frac{x}{x_f}\right]^a=\left(1-b\frac{x}{x_f}\right)^a \quad [B1]$$

where x and x_f are the horizontal coordinate (cm) and wetting front advance (cm), respectively. Then the average soil moisture increase U_0 follows as

$$U_0=\frac{I}{x_f}=\frac{\int_0^{x_f}(\theta-\theta_i)\,dx}{x_f}=\frac{\theta_s-\theta_r}{(a+1)b}\left[1-(1+ab)S_i\right] \quad [B2]$$

where I is the horizontal cumulative infiltration (cm). According to the Boltzmann transformation solution (Philip, 1957b),

$$x = \lambda t^{1/2} \quad [B3]$$

$$I = s t^{1/2} \quad [B4]$$

where λ and s are the Boltzmann variable (cm min$^{-0.5}$) and absorption (cm min$^{-0.5}$), respectively. Substituting Eq. [B2–B4] into Eq. [B1], after rearrangement we have

$$\lambda = \frac{s}{b U_0}\left(1 - S^{1/a}\right) \quad [B5]$$

The flux–saturation relationship equivalent to Eq. [16] is then derived for horizontal absorption as

$$F = \frac{J_w}{J_{w0}} = \frac{\int_{\theta_i}^{\theta} \lambda \, d\theta}{\int_{\theta_i}^{\theta_s} \lambda \, d\theta} = \frac{\left(a + 1 - a S^{1/a}\right) S - (1 + ab) S_i}{1 - (1 + ab) S_i} \quad [B6]$$

Method II

With similar assumptions and derivations as made for Method II for infiltration, we obtain equations equivalent to Eq. [20] and [21] for describing the horizontal soil moisture profile and the average soil moisture increase:

$$\Theta = \frac{\theta - \theta_i}{\theta_0 - \theta_i} = \left(1 - \frac{x}{x_f}\right)^{a_2} \quad [B7]$$

$$U_0 = \frac{I}{x_f} = \frac{\int_0^{x_f} (\theta - \theta_i) \, dx}{x_f} = \frac{\theta_0 - \theta_i}{a_2 + 1} \quad [B8]$$

Following the same process as described above, the flux–saturation relationship, equivalent to Eq. [22], can be obtained as

$$F = \frac{\int_{\theta_i}^{\theta} \lambda \, d\theta}{\int_{\theta_i}^{\theta_s} \lambda \, d\theta} = \Theta\left[1 + a_2\left(1 - \Theta^{1/a_2}\right)\right] \quad [B9]$$

Acknowledgments

This work was supported by the National Natural Science Foundation of China (no. 41271237, 41671228), the National Key Technology Research and Development Program of China (no. 2016YFD0300809, 2016YFD0200107), and the 135 Field Frontier Project of the Institute of Soil Science, CAS (no. ISSASIP1603).

References

Assouline, S. 2013. Infiltration into soils: Conceptual approaches and solutions. Water Resour. Res. 49:1755–1772. doi:10.1002/wrcr.20155

Barry, D.A., J.-Y. Parlange, G.C. Sander, and M. Sivapalan. 1995. Comment on "Explicit expressions for Green–Ampt (delta function diffusivity) infiltration rate and cumulative storage" by G.D. Salvucci and D. Entekhabi. Water Resour. Res. 31:1445–1446. doi:10.1029/95WR00092

Basha, H.A. 2011. Infiltration models for semi-infinite soil profiles. Water Resour. Res. 47:W08516. doi:10.1029/2010WR010253

Boulier, J.F., J. Touma, and M. Vauclin. 1984. Flux-concentration relation-based solution of constant-flux infiltration equation: I. Infiltration into nonuniform initial moisture profiles. Soil Sci. Soc. Am. J. 48:245–251. doi:10.2136/sssaj1984.03615995004800020004x

Brooks, R.H., and A.T. Corey. 1964. Hydraulic properties of porous media. Hydrol. Pap. 3. Colorado State Univ., Fort Collins.

Brutsaert, W. 1976. Concise formulation of diffusive sorption of water in a dry soil. Water Resour. Res. 12:1118–1124. doi:10.1029/WR012i006p01118

Caputo, J.-G., and Y.A. Stepanyants. 2008. Front solutions of Richards' equation. Transp. Porous Media 74:1–20. doi:10.1007/s11242-007-9180-x

Carsel, R.F., and R.S. Parrish. 1988. Developing joint probability distributions of soil water retention characteristics. Water Resour. Res. 24:755–769. doi:10.1029/WR024i005p00755

Dirksen, C. 1975. Determination of soil water diffusivity by sorptivity measurements. Soil Sci. Soc. Am. J. 39:22–27. doi:10.2136/sssaj1975.03615995003900010010x

Evangelides, C., C. Tzimopoulos, and G. Arampatzi. 2005. Flux–saturation relationship for unsaturated horizontal flow. Soil Sci. 170:671–679. doi:10.1097/01.ss.0000185904.72717.4c

Green, W.H., and G.A. Ampt. 1911. Studies on soil physics. J. Agric. Sci. 4:1–24. doi:10.1017/S0021859600001441

Haverkamp, R., J.-Y. Parlange, J.L. Starr, G. Schmitz, and C. Fuentes. 1990. Infiltration under ponded conditions: 3. A predictive equation based on physical parameters. Soil Sci. 149:292–300. doi:10.1097/00010694-199005000-00006

Hogarth, W.L., D.A. Lockington, D.A. Barry, M.B. Parlange, R. Haverkamp, and J.-Y. Parlange. 2013. Infiltration in soils with a saturated surface. Water Resour. Res. 49:2683–2688. doi:10.1002/wrcr.20227

Knight, J.H., and J.R. Philip. 1973. On solving the unsaturated flow equation: 2. Critique of Parlange's method. Soil Sci. 116:407–416. doi:10.1097/00010694-197312000-00003

Kutílek, M. 1980. Constant-rainfall infiltration. J. Hydrol. 45:289–303. doi:10.1016/0022-1694(80)90025-6

Ma, D.H., Q.J. Wang, and M.A. Shao. 2009. Analytical method for estimating soil hydraulic parameters from horizontal absorption. Soil Sci. Soc. Am. J. 73:727–736. doi:10.2136/sssaj2008.0050

Ma, D.H., J.B. Zhang, J.B. Lai, and Q.J. Wang. 2016. An improved method for determining Brooks–Corey model parameters from horizontal absorption. Geoderma 263:122–131. doi:10.1016/j.geoderma.2015.09.007

Ma, D.H., J.B. Zhang, Y.X. Lu, L.S. Wu, and Q.J. Wang. 2015. Derivation of the relationships between Green–Ampt model parameters and soil hydraulic properties. Soil Sci. Soc. Am. J. 79:1030–1042. doi:10.2136/sssaj2014.12.0501

McWhorter, D.B. 1971. Infiltration affected by flow of air. Hydrol. Pap. 49. Colorado State Univ., Fort Collins.

Parlange, J.-Y. 1971. Theory of water-movement in soils.2. One-dimensional infiltration. Soil Sci. 111:170–174. doi:10.1097/00010694-197103000-00004

Parlange, J.-Y. 1975. On solving the flow equation in unsaturated soils by optimization: Horizontal infiltration. Soil Sci. Soc. Am. J. 39:415–418. doi:10.2136/sssaj1975.03615995003900030019x

Parlange, J.-Y., D.A. Barry, M.B. Parlange, W.L. Hogarth, R. Haverkamp, P.J. Ross, et al. 1997. New approximate analytical technique to solve Richards equation for arbitrary surface boundary conditions. Water Resour. Res. 33:903–906. doi:10.1029/96WR03846

Philip, J.R. 1955. Numerical solution of equations of the diffusion type with diffusivity concentration-dependent. Trans. Faraday Soc. 51:885–892. doi:10.1039/tf9555100885

Philip, J.R. 1957a. The theory of infiltration: 1. The infiltration equation and its solution. Soil Sci. 83:345–358. doi:10.1097/00010694-195705000-00002

Philip, J.R. 1957b. The theory of infiltration: 3. Moisture profiles and relation to experiment. Soil Sci. 84:163–178. doi:10.1097/00010694-195708000-00008

Philip, J.R. 1973. On solving the unsaturated flow equation: 1. Flux–concentration relation. Soil Sci. 116:328–335.

Philip, J.R., and J.H. Knight. 1974. On solving the unsaturated flow equation: 3. New quasi-analytical technique. Soil Sci. 117:1–13. doi:10.1097/00010694-197401000-00001

Prevedello, C.L., J.M.T. Loyola, K. Reichardt, and D.R. Nielsen. 2009. New analytic solution related to the Richards, Philip, and Green–Ampt equations for infiltration. Vadose Zone J. 8:127–135. doi:10.2136/vzj2008.0091

Richards, L.A. 1931. Capillary conduction of liquids through porous mediums. Physics 1:318–333. doi:10.1063/1.1745010

Sadeghi, M., A. Tabatabaeenejad, M. Tuller, M. Moghaddam, and S.B. Jones. 2017. Advancing NASA's AirMOSS P-band radar root zone soil moisture retrieval algorithm via incorporation of Richards' equation. Remote Sens. 9:17. doi:10.3390/rs9010017

Šimůnek, J., M.Th. van Genuchten, and M. Šejna. 2005. The HYDRUS-1D software package for simulating the movement of water, heat, and multiple solutes in variably saturated media. Dep. of Environ. Sci., Univ. of California, Riverside.

Smiles, D.E., J.H. Knight, and K.M. Perroux. 1982. Absorption of water by soil: The effect of a surface crust. Soil Sci. Soc. Am. J. 46:476–481. doi:10.2136/sssaj1982.03615995004600030007x

Triadis, D., and P. Broadbridge. 2010. Analytical model of infiltration under constant-concentration boundary conditions. Water Resour. Res. 46:W03526. doi:10.1029/2009WR008181

Triadis, D., and P. Broadbridge. 2012. The Green–Ampt limit with reference to infiltration coefficients. Water Resour. Res. 48:W07515. doi:10.1029/2011WR011747

Valiantzas, J.D. 2010. New linearized two-parameter infiltration equation for direct determination of conductivity and sorptivity. J. Hydrol. 384:1–13. doi:10.1016/j.jhydrol.2009.12.049

van Genuchten, M.Th. 1980. A closed-form equation for predicting the hydraulic conductivity of unsaturated soils. Soil Sci. Soc. Am. J. 44:892–898. doi:10.2136/sssaj1980.03615995004400050002x

Vauclin, M., and R. Haverkamp. 1985. Solutions quasi analytiques de l'équation d'absorption de l'eau par les sols non saturés: II. Problème inverse: Détermination de la diffusivité capillaire. Agronomie 5:607–611. doi:10.1051/agro:19850706

Wang, Q.J., R. Horton, and M.A. Shao. 2002. Horizontal infiltration method for determining Brooks–Corey model parameters. Soil Sci. Soc. Am. J. 66:1733–1739. doi:10.2136/sssaj2002.1733

Wang, Q.J., R. Horton, and M.G. Shao. 2003. Algebraic model for one-dimensional infiltration and soil water distribution. Soil Sci. 168:671–676. doi:10.1097/01.ss.0000095140.68539.8e

White, I. 1979. Measured and approximate flux–concentration relations for absorption of water by soil. Soil Sci. Soc. Am. J. 43:1074–1080. doi:10.2136/sssaj1979.03615995004300060003x

White, I., D.E. Smiles, and K.M. Perroux. 1979. Absorption of water by soil: The constant flux boundary condition. Soil Sci. Soc. Am. J. 43:659–664. doi:10.2136/sssaj1979.03615995004300040006x